AIAA 99-0976

Line-by-Line Infrared Spectra Calculations of Combustion Products Including Doppler Shifts and Vibrational Nonequilibrium

Robert S. Hiers III, J. A. Drakes, W. J. Phillips,
and C. C. Limbaugh
Sverdrup Technology, Inc., AEDC Group
Arnold Engineering Development Center
Arnold Air Force Base, Tennessee 37389

37th AIAA Aerospace Sciences Meeting & Exhibit
January 11-14, 1999 / Reno, NV

AIAA-99-0976

Line-by-Line Infrared Spectra Calculations of Combustion Products Including Doppler Shifts and Vibrational Nonequilibrium*

Robert S. Hiers III,† J. A. Drakes,† W. J. Phillips, and C. C. Limbaugh‡
Sverdrup Technology, Inc., AEDC Group
Arnold Engineering Development Center
Arnold Air Force Base, Tennessee 37389

Abstract

A previously developed line-by-line spectral model has been extended to use the HITRAN and HITEMP line strength data bases. The new spectral model computes the line-by-line spectral radiance and transmittance of homogeneous or inhomogeneous gas paths, including the effects of Doppler shifts due to directed gas velocity and vibrational nonequilibrium. The nonequilibrium vibrational state populations can either be specified directly (perhaps by a state-specific chemistry model, or by imposing rotational and vibrational temperatures for each molecular constituent). Calculations are compared to benchmark laboratory data for hot and hot-through-cold gas paths of CO_2 at high and low spectral resolution. The model showed good agreement with the data, particularly near the line centers. Some discrepancies are noted in the line wings, perhaps indicating a more detailed model of the line wings is needed. Sample calculations demonstrating the effects of directed Doppler shifts and vibrational excitation behind a normal shock are presented.

Introduction

Modeling molecular vibrational relaxation has increased in sophistication in recent years. Techniques have evolved from simple phenomenological models to multi-temperature techniques, to state-to-state chemistry models.[1-3] These state-to-state chemistry models attempt to describe the relaxation process by treating each vibrational state as a separate species and writing the appropriate rate equations for the various energy exchange processes (e.g., V-T or V-V.) In this manner, a distribution of states that is initially described by a Boltzmann distribution will depart from thermodynamic equilibrium when the collision frequency is sufficiently low. This is in contrast to multitemperature models, wherein the vibrational state distribution is assumed to be described by a Boltzmann distribution at one or more temperatures, while the rotational states are in a Boltzmann distribution at another temperature. State-to-state models will eventually serve to validate or disprove the multitemperature approach.

Computing the radiation emitted from these non-Boltzmann distributions requires a radiative transfer model that uses the vibrational/rotational state populations as input. Such a model was developed previously in Ref. 1. In the current work, this line-by-line spectral model[1] has been extended to use the HITRAN[4] and HITEMP[5] molecular line parameter data bases. The new spectral model computes the line-by-line spectral radiance and transmittance of homogeneous or inhomogeneous gas paths, including the effects of vibrational nonequilibrium and Doppler shifts due to directed gas velocity. The nonequilibrium vibrational state populations can either be specified directly through the upper and lower state populations or by specification of rotational and vibrational temperatures for each molecular constituent.

Model Formulation

The HITRAN and HITEMP line strength data files include information on individual vibrational/rotational transitions for 32 diatomic and poly-

* The research reported herein was performed by the Arnold Engineering Development Center (AEDC), Air Force Materiel Command. Work and analysis for this research were performed by personnel of Sverdrup Technology, Inc., AEDC Group, technical services contractor for AEDC. Further reproduction is authorized to satisfy needs of the U. S. Government.

† Senior member, AIAA.

‡ Associate Fellow, AIAA.

atomic molecules. This information includes species and isotope identification, line center frequency, upper and lower quantum numbers and branch assignment, line strength (cm^{-1}/(molecule/cm^2)), and transition moments (R^2 (Debye^2)). As shown in Ref. 1, radiation from a nonuniform NLTE gas at a particular spectral position is given by:

$$N = \left[\int_0^L k^{em}(x) e^{-\int_0^x [k^{em}(x') - k^{abs}(x')]dx'} dx + N_0 \right] e^{-\int_0^L [k^{abs}(x) - k^{em}(x)]dx} \quad (1)$$

where

$$f = 2 \times 10^{-7} hc^2 \omega^3$$

N is the emitted radiance in watts/[cm^2 sr cm^{-1}], N_0 is the incident radiance, the optical frequency ω is in units of wavenumbers (cm^{-1}), Planck's constant (h) has units of erg-sec, the speed of light (c) has units of cm/sec, and k^{abs} and k^{em} (described below) have units of cm^{-1}.

The absorption coefficient is given by:

$$k^{abs}(x) = \frac{8\pi^3 10^{-36}}{3hc} \sum_i A_i \omega_{0i} d_i N_{Li}(x) R_i^2 g_i(\omega, x) \quad (2)$$

where the sum runs over all spectral lines. A_i is the isotopic abundance of the i^{th} line, N_{Li} is the population density (#/cm^3) of the lower nondegenerate rotational-vibrational state, R^2 is the normalized transition moment listed in the HITRAN data base in units of Debye^2, $g_i(\omega)$ is the normalized line shape function in units of cm with a unit integral, and d_i is the degeneracy of the lower rotational-vibrational state. The line shape function (Voigt, Lorentz, etc.) carries an *x* dependency through temperature- and pressure-dependent half widths. The Voigt line shape approximation of Humlicek[6] is used in the current model.

The stimulated emission coefficient is given by:

$$k^{em}(x) = \frac{8\pi^3 10^{-36}}{3hc} \sum_i A_i \omega_{0i} d_i N_{Ui}(x) R_i^2 g_i(\omega, x) \quad (3)$$

where N_{Ui} is the population density of the upper nondegenerate rotational-vibrational state and d_i is the lower state degeneracy factor. Vibrational/rotational nonequilibrium is accounted for through the state populations N_{Ui} and N_{Li}. Doppler shifts due to directed velocity components are accounted for by shifting the line center frequencies (ω_{0i}).

Numerical Method

Equation (1) is the solution of the differential radiative transfer equation

$$\frac{dN}{dx} - N(k^{em} - k^{abs}) = f k^{em} \quad (4)$$

If the gas path is discretized into n homogeneous zones, Eq. (4) may be solved numerically by

$$N_n = \sum_{i=1}^{n} \exp\left[\left(k_i^{em} - k_i^{abs}\right)\delta_i\right] N_{i-1} + \left\{\exp\left[\left(k_i^{em} - k_i^{abs}\right)\delta_i\right] - 1\right\} \frac{f k_i^{em}}{k_i^{em} - k_i^{abs}} \quad (5)$$

where δ_i is the length of the i^{th} zone. The summation is taken over the number of zones.

Benchmark Computations

Carbon dioxide is the only infrared active species considered in this paper. For all the calculations presented below, only the two most common isotopes of CO_2 are considered: $^{16}O^{12}C^{16}O$ (denoted 626) and $^{16}O^{13}C^{16}O$ (denoted 636). The terrestrial abundances of these two isotopes are 0.984260 and 0.01106, respectively. There are 127 CO_2 vibrational states included in the HITEMP data base, with a maximum rotational quantum number (J) of 185. Vibrational state populations for these 127 states were generated from either thermodynamic equilibrium considerations, or by a two-temperature model in which the vibrational and rotational temperatures may be assigned different values. No state-to-state chemistry models were used. This capability will be demonstrated in a later paper.

Comparisons with ERIM Data

Lindquist, et al. of the Environmental Research Institute of Michigan (ERIM) measured the spectral radiance of a hot gas cell, both unattenuated and

attenuated by a cold gas cell.[7] The conditions of the hot cell were 1200 K temperature, 0.10-atm total pressure, 0.01-atm CO_2 partial pressure, and a 0.60-m path length. The conditions of the cold cell were 297 K temperature, 0.13-atm total pressure, 0.115-atm CO_2 partial pressure, and a 100-m path length.

Comparisons of the ERIM hot cell 4.3-μm band data with the line-by-line model calculations are shown in Fig. 1. The spectral resolution of the ERIM data is approximately 4 cm^{-1}. The highly resolved line-by-line calculation results have been convolved with a triangular slit function to attempt to match the spectral resolution of the data. The general level of the data and the calculations compares favorably, with the most disagreement at lower wavenumbers. The shape of the computed band differs significantly from the data in the 2275 cm^{-1} region. This may be due to either missing vibrational/rotational states or transitions in the model. The model allows the influence of each line to extend to 256 half-widths (a typical half-width is 0.07 cm^{-1}). This may be insufficient in some regions. The disagreement in the low wavenumber wing of the band is most likely due to this treatment of the long tail of each individual line or missing vibrational bands.

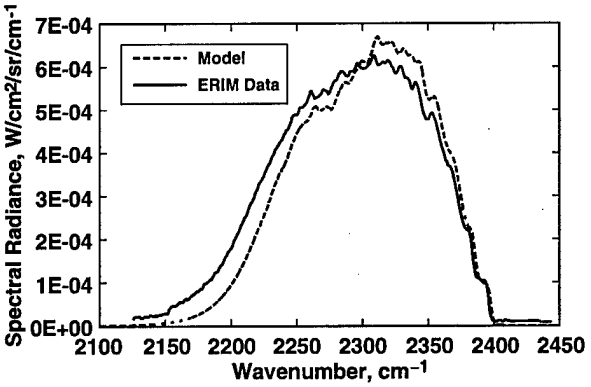

Fig. 1. Comparison of ERIM hot cell data with model results.

Comparisons of the ERIM hot-through-cold cell 4.3-μm band data with the line-by-line model calculations are shown in Fig. 2. The model correctly computes the location of the typical blue and red spikes at approximately 2400 and 2195 cm^{-1}, respectively. The blue spike radiance calculations are about a factor of 6 above the data. It should be noted that the signal-to-noise ratio of the data is very poor in this region. The disagreement in the computed signal levels in the red spike region is probably due to the treatment of the line tails or missing vibrational bands.

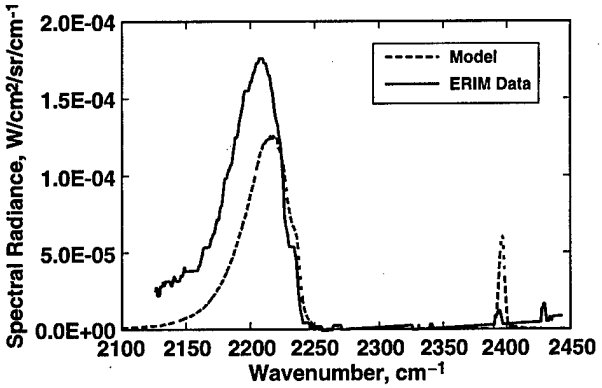

Fig. 2. Comparison of ERIM hot-through-cold cell data with model results.

Comparisons with AEDC Data

Phillips[8] measured the high-temperature transmittance of CO_2 gas paths at a spectral resolution of approximately 0.016 cm^{-1}. These experiments were conducted at the U.S. Air Force Arnold Engineering Development Center (AEDC). The experimental conditions were 1000 K temperature, 0.013-atm total pressure, 0.0013-atm CO_2 partial pressure, and a 10.6-cm path length. The line-by-line calculation results have been convolved with a triangular slit function to attempt to match the spectral resolution of the data. A comparison of the model results and the AEDC data in the 2360 cm^{-1} spectral region is shown in Fig. 3. The computed transmittance agrees very well with the data near the line centers, but the agreement is not as good

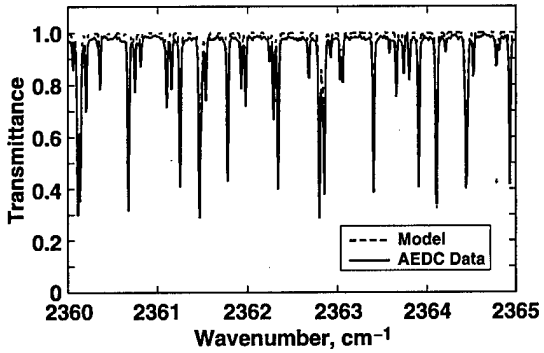

Fig. 3. Comparison of AEDC hot cell data with model results.

in the wings. This overprediction of transmittance is probably due to the treatment of the line tails described above. The direct extension of the region of influence of each spectral line is extremely computationally expensive. This is why models such as the Fast Atmospheric Signature Code (FASCODE)[9] use an approximate treatment of the wings. It should also be noted that the measurement of these very high transmittances is difficult due to source intensity drift with time as well as other factors, leading to relatively low signal to noise in these spectral regions. This may also contribute to the disagreement between the model and data in the high transmittance regions. Figure 4 shows a comparison of the data and model over a 1-cm^{-1}-wide spectral region. Note again the excellent agreement near the line centers.

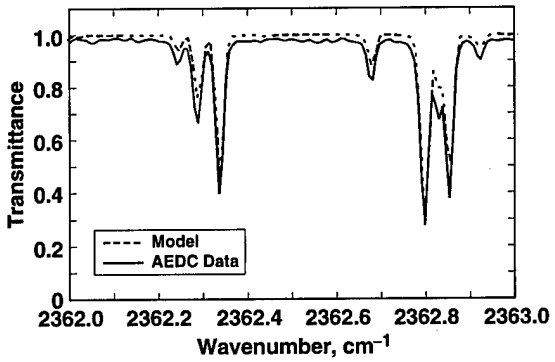

Fig. 4. Comparison of AEDC hot cell data with model results over a narrow spectral region.

Effect of Doppler Shift

Directed velocity (as opposed to random, thermal velocity) causes the line center locations to shift due to the Doppler effect. A sample two-zone calculation was done to demonstrate this. The conditions in each zone are: 1000 K temperature, 0.013-atm total pressure, 0.0013-atm CO_2 partial pressure, and a 5.3-cm path length. Thermodynamic equilibrium is assumed. The gas in one zone is moving at 1.5 km/sec towards the observer, while the gas in the other zone is moving at 1.5 km/sec away from the observer. This can be regarded as a simplistic model for the radial velocity distribution in a rocket nozzle. This velocity will cause the line centers in the zone moving towards the observer to be shifted approximately 0.01 cm^{-1} to the blue, while the line centers in the zone moving away from the observer will be shifted a like amount to the red. Note that the total gas path is the same as that used in the Phillips/AEDC experiment above. This allows the unshifted and shifted computed spectra to be compared. These comparisons appear in Figs. 5 and 6. Figure 5 compares the computed transmittance with and without the Doppler shift over the same 1-cm^{-1}-wide spectral region as seen in Fig. 4. Figure 6 shows the comparison of the same results over a narrower spectral region. The splitting of the spectral lines due to the Doppler shift is readily apparent.

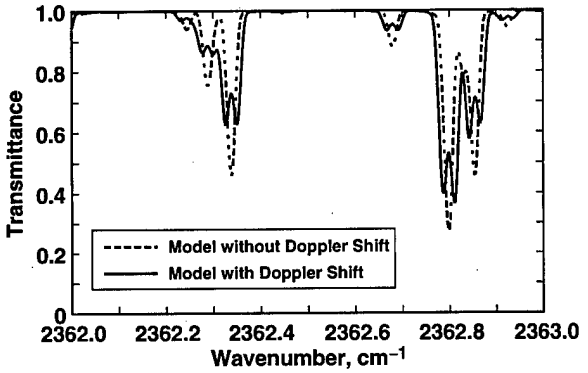

Fig. 5. Comparison of model results with and without Doppler shift.

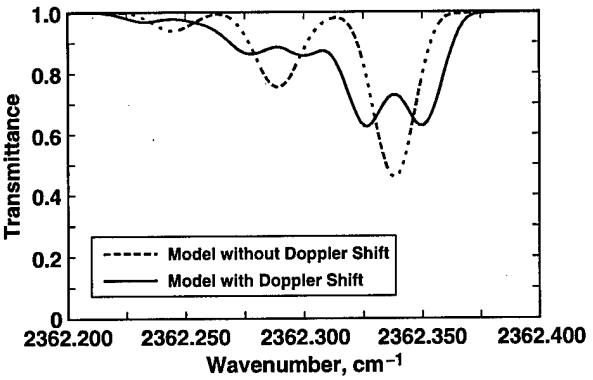

Fig. 6. Comparison of model results with and without Doppler shift over a narrow spectral region.

Vibrational Excitation Behind a Normal Shock

A simplistic treatment of the vibrational excitation behind a normal shock is seen in Fig. 7. The conditions for these calculations are shown in Table 1. The vibrational populations are assumed to be initially frozen at the upstream condition when they first cross the shock. The vibrational populations then approach equilibrium with the rotational

states. No explicit relaxation calculation was performed. The vibrational temperatures in Table 1 are assumed to exist at some location downstream of the shock. The rotational temperature is assumed to be in equilibrium with the translational temperature at all conditions. The ambient gas is assumed to be air, containing 30 ppm CO_2. The path length is held fixed at 8 cm. The three vibrational modes of CO_2 (bending, symmetric stretch, and asymmetric stretch) were assumed to be in equilibrium. Future work will use both multitemperature and state-to-state approaches for this flow field.

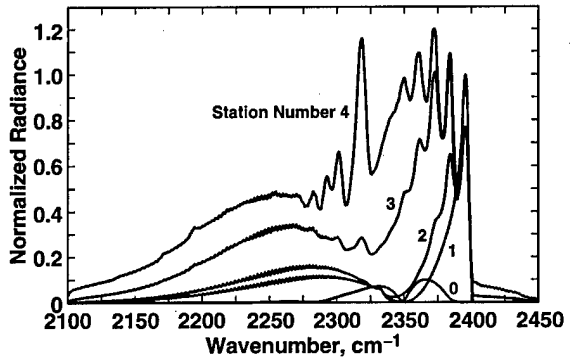

Fig. 7. Vibrational relaxation behind a normal shock.

Table 1. Conditions for Normal Shock Calculations

Parameter	Upstream Conditions	Downstream Conditions			
Station Number	0	1	2	3	4
Mach Number	9.8	0.29	0.29	0.29	0.29
Pressure, atm	0.01	1.14	1.14	1.14	1.14
T_{rot}, K	300	3000	3000	3000	3000
T_{vib}, K	300	300	1000	2000	3000

The results of these calculations are shown in Fig. 7. The results have been normalized so that the change in vibrational structure can be seen in a single plot. The increasing vibrational excitation as the vibrational temperature approaches the rotational temperature is readily apparent. The drastic change in the band profile as equilibrium is approached should be experimentally observable. More detailed flow-field and relaxation calculations would be required to compute physically realistic spectra.

Summary and Recommendations

A previously developed line-by-line spectral model has been extended to use the HITRAN and HITEMP line strength data bases. The new spectral model computes the line-by-line spectral radiance and transmittance of homogeneous or inhomogeneous gas paths, including the effects of Doppler shifts due to directed gas velocity and vibrational nonequilibrium. The nonequilibrium vibrational state populations can either be specified directly (perhaps by a state-specific chemistry model, or by imposing rotational and vibrational temperatures for each molecular constituent). Model results were compared to benchmark laboratory data for hot and hot-through-cold gas paths of CO_2 at high and low spectral resolution. The model compared favorably to the data in most cases. However, it does appear that the treatment of the line tails is inadequate to capture some features. This deficiency will be addressed in later versions of the model. The effect of Doppler shifts was demonstrated in a sample calculation with directed velocity components on the order of that expected in rocket nozzle exhausts. Line splitting was clearly visible in the results. A simplistic model of vibrational excitation behind a normal shock was presented, demonstrating the ability of the model to use a multitemperature description of the vibrational/rotational populations. The ability of the spectral model to interface with state-to-state vibrational chemistry models will be presented in a later paper.

References

1. Limbaugh, C. C., Hiers, R. S. III, and Phillips, W. J., "High-Resolution Spectral Diagnostics in Flows with Mild Vibrational Relaxation," AIAA-89-1676, AIAA 24th Thermophysics Conference, Buffalo, NY, June 12-14, 1989.

2. Limbaugh, C. C., Tramel, R. A., Drakes, J. A., and Hiers, R. S. III, "Analysis of CO_2 Vibronic Ensembles in Nonequilibrium Combustion Flows," AIAA-94-1985, 6th AIAA/ASME Joint Thermophysics and Heat Transfer Conference, Colorado Springs, CO, June 20-23, 1994.

3. Limbaugh, C. C. and Drakes, J. A., "CO_2 Vibrational Relaxation Effects in a Laser-Heated Hypersonic Flow," AIAA 97-2492, 32nd Thermophysics Conference, Atlanta, GA, June 23-25, 1997.

4. Rothman, L. S., et al., "The HITRAN database: 1986 edition," *Applied Optics*, Vol. 26, No. 19, 1 October 1987, pp. 4058.

5. Rothman, L. S., et al., "HITEMP, the High Temperature Molecular Spectroscopic Database," Special HITRAN issue, *Journal of Quantitative Spectroscopy and Radiative Transfer*, to be published.

6. Humlicek, J., "Optimized Computation of the Voigt and Complex Probability Functions," *Journal of Quantitative Spectroscopy and Radiative Transfer*, Vol. 27, No. 4, 1982, pp. 437-444.

7. Lindquist, G. H., et al., "Experimental and Analytical Investigation of Hot Gas Emission Attenuated by Cold Gases - Atmospheric Absorption Applied to Plume Emission," AFRPL-TR-75-30, August 1975.

8. Phillips, W. J., "Band-Model Parameters for the 4.3-μm CO_2 Band in the 300-1000 K Temperature Region," *Journal of Quantitative Spectroscopy and Radiative Transfer*, Vol. 48,1992, p. 91.

9. Clough, S. A,. et al., "ITS 88: Current Problems in Atmospheric Radiation," J. Lenoble and J. F. Gelewn, ed., Deepak Publishing, Hampton, VA, May 1989.